A Generalized Method to Investigate the Bistability of Curved Beams using Buckling Analysis

Safvan P[*, 1], Darshan S[*, 2], Anirudh N Katti[*, 3], G.K.Ananthasuresh[*, 4]

Abstract

In this paper, an initially straight beam with torsional springs at its two hinged ends is subjected to an axial force and its buckling mode shapes are found. Any shape which is a linear combination of the modes is taken as the as-fabricated stress-free form and then subjected to a transverse actuating force. Post-buckling analysis is used to compute the force-displacement characteristic of such a beam and thereby check if bistability exists. Two special cases of the torsion spring constants being very large and zero are presented. The former is a known result where a cosine curve is the fundamental buckling mode that does not give bistability unless its asymmetric second mode shape is avoided by a physical constraint. When the spring constant is zero, a single sine curve profile, which is the fundamental mode, can be made bistable without having to physically constrain the asymmetric buckling modes. This is realized when pinned-pinned boundary condition is used, which further allows the element to have enhanced range of travel between its two stable states, reduced switching force, and provision for secondary lateral actuation. To realise a monolithic compliant bistable element without any kinematic joints, torsion springs are substituted with equivalent revolute flexures. Physical embodiments of three types of bistable curved beams, namely, fixed-fixed, pinned-pinned, and revolute flexure-based, are presented.

Keywords: Fully-compliant mechanisms, revolute flexures, buckling modes

1 Introduction

Mechanisms which have two force-free stable equilibrium positions in their range of motion are called bistable mechanisms. Their characteristic force and energy graphs are shown in Fig. 1. Bistable mechanisms are used in both macro-scale and micro-scale applications. Relays [1][2], micro-actuators [3] micro-valves [4] and mechanical memory components [5] are examples of bistable micro devices. Circuit breakers, switches, easy-chairs [6] and rear trunk lids of cars [7] are examples of macro-scale bistable devices. In this paper we present a generalized method to investigate the bistability of curved beams and to design monolithic fully-compliant bistable mechanisms with enhanced performance.

One way to obtain bistability in curved beams is to use linear combinations of buckling mode shapes of a straight beam. Most bistable mechanism reported in the literature employ fixed-fixed boundary conditions. For fixed-fixed boundary conditions, the mode shapes of a straight beam are as shown in Fig. 2. If the first cosine buckling mode shape is used as the bistable mechanism's as-fabricated shape, Qui et at. [8] proved that the mechanism does not exhibit bistability unless its

_____

[*] Department of Mechanical Engineering, Indian Institute of Science, Bengaluru, India

[1] Email: safvan@mecheng.iisc.ernet.in

[2] Email: darshan.sheshgiri@gmail.com

[3] Email: anirudhkatti@gmail.com

[4] (Corresponding author) Email: suresh@mecheng.iisc.ernet.in

asymmetric second mode shape is prevented by a physical constraint. They proposed a monolithic compliant bistable mechanism that uses two cosine curved centrally-clamped parallel beams shown in Fig. 3 as its as-fabricated shape. Such a shape is given by

$$\bar{w} = \frac{h}{2}\left[1 - \cos\left(\frac{2\pi x}{L}\right)\right] \tag{1}$$

where h is the apex height of the beam and L distance between the ends.
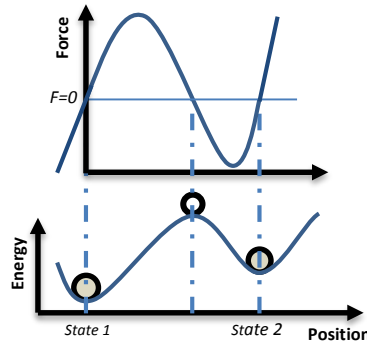
Fig. 1. Bistable mechanism force and energy behaviour
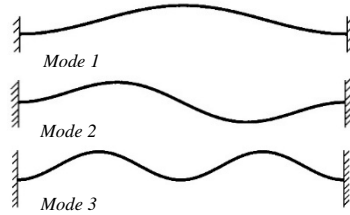
Fig. 2. Fixed-fixed boundary condition mode shapes

Fig. 3. Two cosine curved centrally-clamped parallel beams bistable mechanism

On the other hand, if pinned-pinned boundary conditions are used, the modes shapes are as shown in Fig. 4. A single sine curve profile, which is the fundamental mode, can be made bistable without having to physically constrain the asymmetric buckling modes. It is given by

$$\bar{w} = h \sin\left(\frac{\pi x}{L}\right) \tag{2}$$

A bistable curved beam with pinned-pinned boundary conditions possesses advantages over the curved fixed-fixed beam. They have enhanced range of travel between its two stable states, reduced switching force, and provision for secondary lateral actuation. However, pin joints at micro scale lead to difficulties in manufacturing and problems in operation due to friction and wear. Therefore, the intermediate case of hinged ends with rotational flexures is an option worth

exploring. This approach, as demonstrated in this paper, gives rise to hinge-free monolithic designs while retaining the aforementioned three advantages.
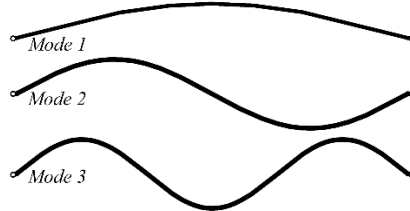
Fig. 4. Pinned-pinned boundary condition mode shapes

In this paper, we propose to replace the pin joints with compliant revolute joints. Towards this, a bistable element is designed by following a systematic buckling analysis-based procedure. The torsional stiffness is lumped into a torsion spring at the revolute joint for the purposes of modelling. The buckling mode shapes for such a beam are found in Section 2. The as-fabricated profile is taken as a linear combination of the buckling modes. The potential energy of the system is found and minimized with respect to mode weights to obtain the force-displacement relationship, which can be used to check if the mechanism is bistable. In Section 3, we present designs of three types of bistable elements, namely, fixed-fixed, pinned-pinned, and revolute flexure-based.

2 Analysis of the beam with general boundary conditions

2.1 Buckling Analysis

The governing differential equation for a generally constrained beam shown in Fig. 5, subjected to axial load P is given by

$$EI\frac{d^4w}{dx^4} + P\frac{d^2w}{dx^2} = 0 \tag{3}$$

where w is the transverse displacement of the beam perpendicular to the axial force, E is the Young's modulus of the material, and I is area moment of inertia of the cross-section of the beam. Further, the length of the beam is L, the axial force P and the torsional spring constant is κ.

Fig. 5. A generally constrained beam subjected to axial force

We use the notation M to condense the force, material property and cross-section property. Note that M here does not stand for the bending moment.

$$M = \sqrt{\frac{P}{EI}} \tag{4}$$

The solution to Eq. (3) is of the form

$$\frac{d^2w}{dx^2} = A\cos(Mx) + B\sin(Mx) \tag{5}$$

By integrating twice, we get

$$w = -\frac{A}{M^2}\cos(Mx) - \frac{B}{M^2}\sin(Mx) + Cx + D \tag{6}$$

where A, B, C and D are constants. The boundary conditions are given by

$$w|_{x=0} = w|_{x=L} = 0 \tag{7}$$

$$EI\frac{d^2w}{dx^2}\bigg|_{x=0} = \kappa\frac{dw}{dx}\bigg|_{x=0} \quad , \quad EI\frac{d^2w}{dx^2}\bigg|_{x=L} = \kappa\frac{dw}{dx}\bigg|_{x=L} \tag{8}$$

By applying the boundary conditions in Eq. (5) and Eq. (6), we get

$$C = \frac{EIA}{\kappa} + \frac{B}{M}$$
$$D = \frac{A}{M^2} \tag{9}$$

Using Eqs. (5), (6), (7), (8) and (9) to reduce to a system of two equations in two unknowns A and B gives rise to

$$\begin{bmatrix} -\dfrac{\cos(ML)}{M^2} + \dfrac{1}{M^2} + \dfrac{EIL}{\kappa} & -\dfrac{\sin(ML)}{M^2} + \dfrac{L}{M} \\ \cos(ML) - \dfrac{\kappa\sin(ML)}{MEI} - 1 & \sin(ML) + \dfrac{\kappa\cos(ML)}{MEI} - \dfrac{\kappa}{MEI} \end{bmatrix} \begin{Bmatrix} A \\ B \end{Bmatrix} = \begin{Bmatrix} 0 \\ 0 \end{Bmatrix} \tag{10}$$

For a non-trivial solution, we equate the determinant of the matrix in Eq. (10) to zero, which yields the condition:

$$\sin\left(\frac{ML}{2}\right)\left[\cos\left(\frac{ML}{2}\right)\left\{\frac{E^2I^2L}{\kappa^2} + \frac{L}{M^2}\right\} - \frac{2}{M^3}\sin\left(\frac{ML}{2}\right)\right] = 0 \tag{11}$$

Eq. (11) can be used to find the buckling mode shapes. For $\kappa = 0$, the mode shapes are the sine mode shapes as shown in Fig. 4. For $\kappa = \infty$, the mode shapes are the cosine mode shapes as shown in Fig. 2. For intermediate values, with geometric and material parameters shown in Table 1, the buckling mode shapes are as shown in Fig. 6. Here b is the out-of-plane depth of the beam and t is the thickness of the beam.

Table 1. Geometric and material parameters of a beam

S.No.	Parameter	Value
1	L	0.125 m
2	b	0.005 m
3	t	0.001 m
4	E	2.1 GPa
5	h	0.011 m

a. $\kappa = 0.00525$ Nm/rad

b. $\kappa = 0.01$ Nm/rad

c. $\kappa = 0.2$ Nm/rad
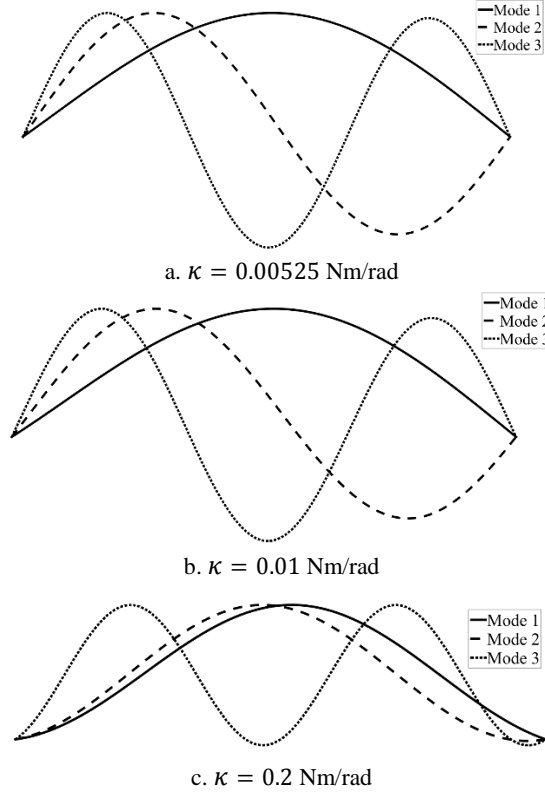
Fig. 6. Buckling mode shapes for a beam with different torsional stiffness values

For $\kappa > 0.503$ Nm/rad, the mode shapes closely resemble those of fixed-fixed boundary condition. For $\kappa < 0.01$ Nm/rad, the mode shapes closely resemble those of pinned-pinned boundary condition.

2.2 Post-buckling analysis

Any shape which is a combination of the buckling modes can be taken as the as-fabricated shape of the bistable element ($\overline{w}$). When the element of such a shape is subjected to a transverse force, it may or may not exhibit bistability. We now discuss a method to check for the bistability.

The buckling mode shapes found in Section 2.1 are orthonormal to one another. They form the basis vectors for the given torsional stiffness, i.e., any shape can be written as a linear combination of these basis vectors. Hence, the deformed shape of the bistable beam can also be written as a linear combination of the basis vectors. For simplicity, we will first assume the deformed shape (w) of the beam to be a linear combination of the first two mode shapes, i.e.

$$w = A_1 w_1 + A_2 w_2 \tag{11}$$

where A_1 and A_2 are the mode weights. In order to determine the force-displacement curve of the bistable element, we will minimize the potential energy of the system with respect to both A_1 and A_2. The potential energy is given by

5

$$PE = SE_b + SE_c - WP_f + \frac{1}{2}\kappa\left(\frac{dw}{dx}\Big|_{x=0}\right)^2 + \frac{1}{2}\kappa\left(\frac{dw}{dx}\Big|_{x=L}\right)^2 \tag{12}$$

where SE_b is the strain energy associated with the bending of the element, SE_c is the strain energy associated with deformation due to compression and WP_f is the work potential due to transverse force f. When more than one beam element is used, the bending energy and compression energy for each element has to be accounted for. The work potential term however, remains the same. For example, in the two cosine curved mechanism (Fig. 3), an additional $SE_b + SE_c$ should be added to Eq. (13) as there are two beam elements. SE_b and SE_c for a single beam element are given by

$$SE_b = \frac{EI}{2}\int_0^L \left(\frac{d^2\overline{w}}{dx^2} - \frac{d^2w}{dx^2}\right)^2 dx \tag{13}$$

$$SE_c = -\frac{L^2 bt}{I}\left(s - \frac{s^2}{2\overline{s}} - \frac{\overline{s}}{2}\right)$$

$$s = \int_0^L \sqrt{1 + \left(\frac{dw}{dx}\right)^2}\, dx \approx \int_0^L \left(1 + \frac{1}{2}\left(\frac{dw}{dx}\right)^2\right) dx \tag{14}$$

$$\overline{s} = \int_0^L \left(1 + \frac{1}{2}\left(\frac{d\overline{w}}{dx}\right)^2\right) dx$$

$$WP_f = -fd \tag{15}$$

$$d = \overline{w}\left(\frac{L}{2}\right) - w\left(\frac{L}{2}\right) \tag{16}$$

For static equilibrium, we have:

$$\frac{\partial(PE)}{\partial A_1} = 0 \tag{17}$$

$$\frac{\partial(PE)}{\partial A_2} = 0 \tag{18}$$

Equations (17), (18) and (19) become a system of three equations in three unknowns: f, A_1 and A_2. There are two possible solutions to this system: one when the energy of the system does not equal the energy of the second buckling mode, and the other when it does. Solving both numerically gives the force-displacement curve. Similarly, when we consider more than two mode shapes, we get additional equations to solve.

2.3 An illustrative example

To illustrate the method, we consider the split-tube flexure described in [9] where torsional stiffness is $\kappa = 0.00525$. The mode shapes can be found using Eq. (11) are shown in Fig. 6a. The as-fabricated shape is taken to be the first mode. For the first mode, the values of constants in Eq. (6) are given by

$$A = 0.2205, B = -1.0000, C = -0.002, D = 0.0003, M = 27.1263 \tag{19}$$

Then Eq. (6) becomes

$$w = (2.9887\cos(27.1623x) + 14\sin(27.1623x) - 20x + 3)10^{-4} \tag{20}$$

Removing the constant terms and modifying the equation such that h would be the apex height in meters, the equation of the as-fabricated shape of the bistable element is given by

$$\bar{w} = h(-0.1918\cos(27.1623x) + 0.8699\sin(27.1623x) - 1.2836x + 0.1925) \quad (21)$$

The bistable element is shown in Fig. 7 and the force-displacement curve is shown in Fig. 8. Fig. 8 shows a curve and a straight line, corresponding the two solutions discussed in the end of Section 2.2. As the element is deformed, it travels along the curve until it reaches the dotted line, corresponding to the second buckling mode, as shown in Fig. 8a. At the point the curve intersects the straight line, it deforms into the second buckling mode shape (Fig. 8b). It then travels along the straight line till it once again intersects the curve. At this point, the element returns to the first buckling mode shape (Fig. 8c) and reaches the second equilibrium state. Hence, the actual force-displacement curve is a hybrid that switches between the curve and the straight line at the intersections. It should be observed in Fig. 8c, that the point at which the element returns to the first buckling mode is below the zero force line, and hence, the element is bistable. If on the other hand, the intersection point was above the zero-force line, the mechanism would bounce back when the actuating force is released, and hence, wouldn't be bistable.
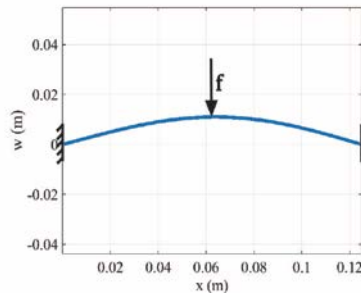
Fig. 7. Bistable element using the first mode shape as the as-fabricated shape for $\kappa = 0.00525$
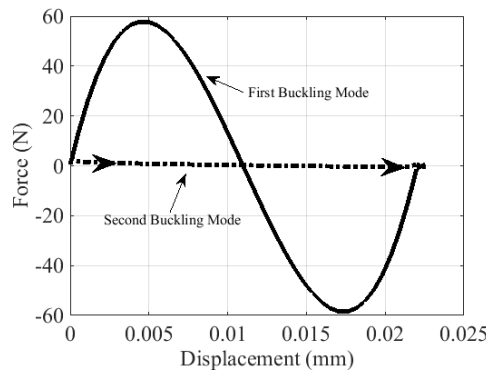
a. Hybrid force-displacement curve for both solutions

7
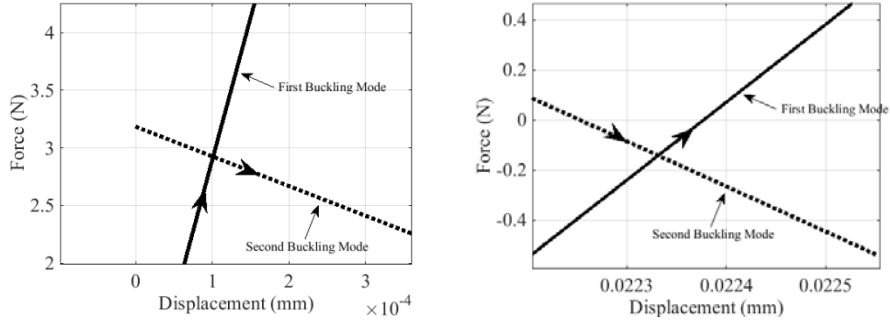
b. Enlarged view of the first intersection where element switches to second mode

c. Enlarged view of the second intersection where element returns to first mode

Fig. 8. Force-displacement curve for the bistable element using the first mode shape as the as-fabricated shape for $\kappa = 0.0052$

3   Examples of bistable mechanisms synthesized

The methodology described in Section 2 is used to synthesize bistable mechanisms for different values of torsional stiffness. All the designs shown use the geometric and material properties shown in Table 1. Fig. 9a shows a single cosine curve mechanism for fixed-fixed boundary conditions. As seen in force-displacement curve, the curve is only marginally below the zero-force line. A small disturbance would be enough to switch it back to the first stable state. On the other hand, force-displacement curve in Fig. 9b for the two cosine curved centrally-clamped parallel beam mechanism for fixed-fixed boundary condition is clearly bistable. .

$$\overline{w} = \frac{h}{2}\left[1 - \cos\left(\frac{2\pi x}{L}\right)\right]$$

$$\overline{w} = \frac{h}{2}\left[1 - \cos\left(\frac{2\pi x}{L}\right)\right]$$
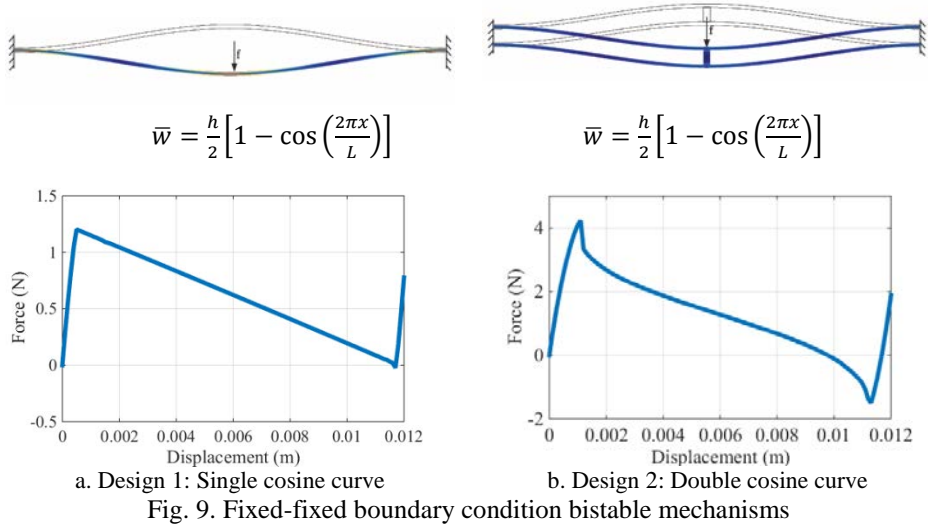
a. Design 1: Single cosine curve   b. Design 2: Double cosine curve

Fig. 9. Fixed-fixed boundary condition bistable mechanisms

Fig. 10 shows bistable mechanisms for pinned-pinned boundary conditions. Here, single curved beams can be made bistable without the necessity to physically constraint the asymmetric mode. As seen, compared to the fixed-fixed case, the deformed plot and the force-displacement graphs show enhanced range of travel

between its two stable states and reduced switching force. Fig. 10b shows the optimized bistable curve for pinned-pinned boundary condition. Optimization was carried for maximum range of travel for a given actuation force taking first three mode weights, A_1, A_2 and A_3, as the design variables.

$$\bar{w} = h \sin\left(\frac{\pi x}{L}\right)$$

$$\bar{w} = 33.8\left\{0.4634 \sin\left(\frac{\pi x}{L}\right) + 0.0653 \sin\left(\frac{3\pi x}{L}\right) - 0.0724 \sin\left(\frac{5\pi x}{L}\right)\right\}$$

a. Design 1: Sine curve   b. Design 2 : Optimized curve
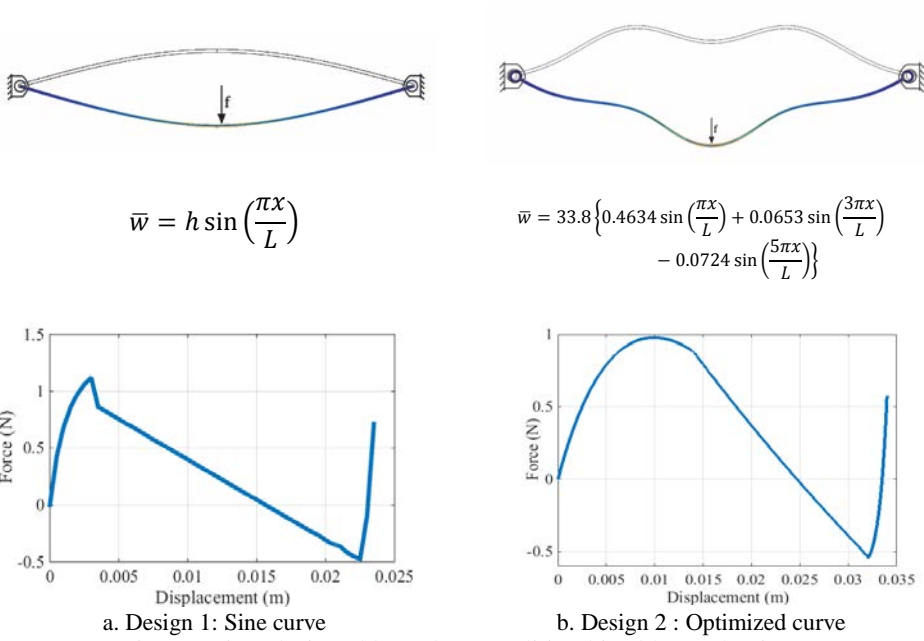
Fig. 10. Pinned-pinned boundary condition bistable mechanisms

Prototypes of the mechanisms shown in Fig. 9 and Fig. 10 are shown in Fig. 11. Fig. 11a is the single cosine curve mechanism with fixed-fixed boundary condition. This mechanism isn't bistable and hence has only one state. Fig. 11b is the double cosine curve mechanism with fixed-fixed boundary condition. This mechanism is bistable. We measure the apex height h and the travel t_r in each mechanism. As h could be different in the prototypes, the ratio $\frac{t_r}{h}$ is an indicative of the travel between the two states factoring in the apex height. The greater the ratio, the greater the travel.

a. Fixed-fixed single cosine curve monostable mechanism

Prototype in state 1   Prototype in state 2

b. Fixed-fixed double cosine curve mechanism [8] $\left(\frac{t_r}{h} = \frac{18}{11} = 1.64\right)$

Prototype in state 1   Prototype in state 2

c. Pinned-pinned sine curve mechanism $\left(\frac{t_r}{h} = \frac{21}{11} = 1.90\right)$
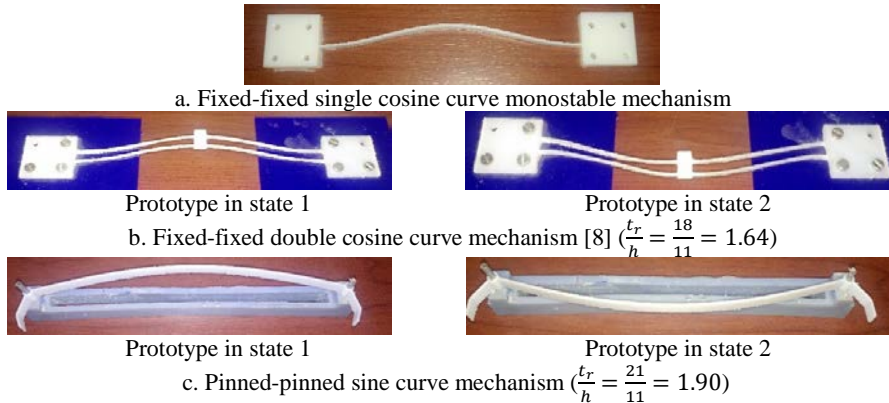
Prototype in state 1   Prototype in state 2

d. Pinned-pinned first three sine modes linear combination mechanism ($\frac{t_r}{h} = \frac{30}{11} = 2.72$)

Fig. 11. Fixed-fixed and pinned-pinned bistable mechanisms

In Fig. 11c, the sine curve mechanism is shown. In this mechanism, the pin joints are used to add an appendage which would allow for lateral actuation. Fig. 11d shows an optimized mechanism for pinned-pinned boundary condition. This mechanism has the largest $\frac{t_r}{h}$ ratio.

Fig. 12 shows a bistable mechanism with revolute flexures. The basic shape used is a cosine curve. Revolute flexures at both ends prevent axial motion but allow rotation. As with the case with pinned-pinned boundary conditions, the deformed shape and the force-displacement curve show enhanced range of travel between its two stable states and reduced switching force compared to the fixed-fixed case.
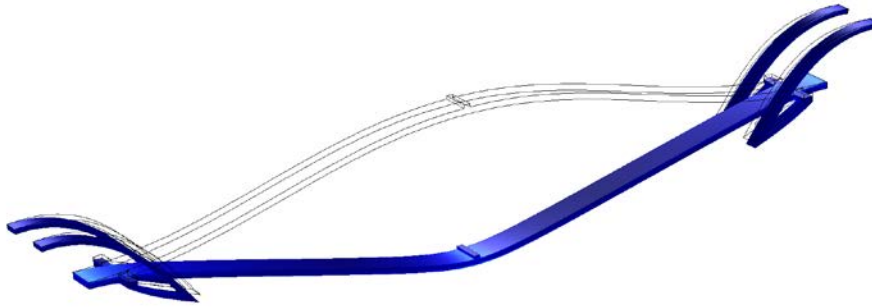
a. Deformation plot of the mechanism
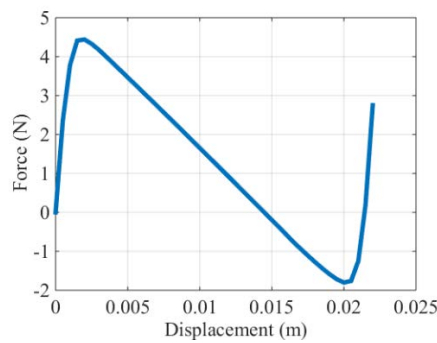
b. FEA force-displacement curve

c. Prototype in state 1

d. Prototype in state 2

Fig. 12. Prototype of revolute flexure bistable mechanisms ($\frac{t_r}{h} = \frac{17}{8} = 2.215$)

4   Conclusions

This paper proposed a methodology to investigate bistable mechanisms with compliant revolute flexures at both ends and to aide in their design. The flexures, being close to pinned-pinned boundary allow for the design of efficient bistable mechanisms, i.e., they allow the element to have enhanced range of travel between its two stable states, reduced switching force, and provision for secondary lateral actuation. Based on the analysis, we have synthesised and presented bistable mechanisms: two for pinned-pinned boundary condition and one with revolute flexures.

Acknowledgement

References

[1] Qiu, Jin, Jeffrey H. Lang, Alexander H. Slocum, and Alexis C. Weber. "A bulk-micromachined bistable relay with U-shaped thermal actuators", Journal of Microelectromechanical Systems, No. 5, 2005, pg 1099-1109

[2] Troy Gomm, Larry L Howell and Richard H Selfridge, "In-plane linear displacement bistable microrelay", Journal of Micromechanics and Microengineering, Vol. 12, 2002, Pages 257-264

[3] Matoba, Hirotsugu, Toshio Ishikawa, Chang Jin Kim, and Richard S. Muller. "A bistable snapping microactuator." In *Micro Electro Mechanical Systems, 1994, MEMS'94, Proceedings, IEEE Workshop on*, pp. 45-50. IEEE, 1994.

[4] Rajesh Luharuka and Peter J Hesketh , "A bistable electromagnetically actuated rotary gate microvalve", Journal of Micromechanics and Microengineering, Vol. 18, 2008, doi:10.1088/0960-1317/18/3/035015

[5] Hälg, B. "On a nonvolatile memory cell based on micro-electro-mechanics." In/Micro Electro Mechanical Systems, 1990. Proceedings, An Investigation of Micro Structures, Sensors, Actuators, Machines and Robots. IEEE/, pp. 172-176. IEEE, 1990

[6] S Darshan, T.J.Lassche, J.L.Herder, G.K.Ananthasuresh, "A Compliant Two-Port Bistable Mechanism with Application to Easy-Chair Design", 14th World Congress in Mechanism and Machine Science, Taipei, Taiwan, October 25-30, 2015

[7] Zhang, Shouyin, Guimin Chen, "Design of compliant bistable mechanism for rear trunk lid of cars", Intelligent Robotics and Applications, Springer Berlin, Heidelberg, pp291-299, 2011

[8] Jin Qiu, Jeffrey H. Lang, Alexander H. Slocum, "A Curved-Beam Bistable Mechanism", Journal of Microelectromechanical Systems, Vol. 13, No. 2, April 2004, pg 137-146

[9] Goldfarb, Michael, and John E. Speich. "A well-behaved revolute flexure joint for compliant mechanism design." *Journal of Mechanical Design* 121.3 (1999): 424-429.